

This is a pre print version of the following article:

Pullout behavior of polypropylene macro-synthetic fibers treated with nano-silica / DI MAIDA, Pietro; Radi, Enrico; Sciancalepore, Corrado; Bondioli, Federica. - In: CONSTRUCTION AND BUILDING MATERIALS. - ISSN 0950-0618. - ELETTRONICO. - 82:(2015), pp. 39-44. [10.1016/j.conbuildmat.2015.02.047]

*Terms of use:*

The terms and conditions for the reuse of this version of the manuscript are specified in the publishing policy. For all terms of use and more information see the publisher's website.

23/06/2024 22:16

(Article begins on next page)

# Pullout behavior of polypropylene macro-synthetic fibers treated with nano-silica

P. Di Maida<sup>a</sup>, E. Radi<sup>a,\*</sup>, C. Sciancalepore<sup>b</sup>, F. Bondioli<sup>c</sup>

<sup>a</sup>*Dipartimento di Scienze e Metodi Dell'ingegneria - Università di Modena e Reggio Emilia*

<sup>b</sup>*Dipartimento di Ingegneria "Enzo Ferrari" - Università di Modena e Reggio Emilia*

<sup>c</sup>*Dipartimento di Ingegneria Industriale - Università di Parma*

**Abstract:** A study of the effects of nano-silica treatment on the bonding properties of macro synthetic polypropylene fibers embedded in a cement matrix is provided in the present paper as a step to improve interfacial properties of the fiber reinforced cementitious composites (FRCC). Polypropylene fibers were treated by sol-gel technique, allowing to obtain a nano-silica coating. Scanning electron microscopy was used to observe the morphological features of PP fibers surfaces before and after the pullout test. The effects of the treatment were investigated by comparative pullout tests on treated and untreated fibers. An increase in maximum load and energy necessary for the complete extraction of the fiber was observed, as a consequence of the improvement of the interface properties due to the nano-silica hydration activity. These two parameters control the crack-resistance and ductility properties of FRCC and are deeply influenced by bonding and friction phenomena. The hydration products act as chemical and physical anchors, thus producing a densification of the interface transition zone. The abrasion phenomena occurring on the fiber surface during the pullout test are responsible of hardening behavior, consisting in the increase in the frictional shear stress with the fiber slip and thus in the energy required for fiber extraction.

**Keywords:** fiber reinforced cementitious composites, macro synthetic fibers, polypropylene, nano-silica, pullout behavior.

\* Corresponding author. Tel.:+39 0522 522221; fax:+39 0522 522609.  
E-mail address: enrico.radi@unimore.it (E. Radi).

## 1. INTRODUCTION

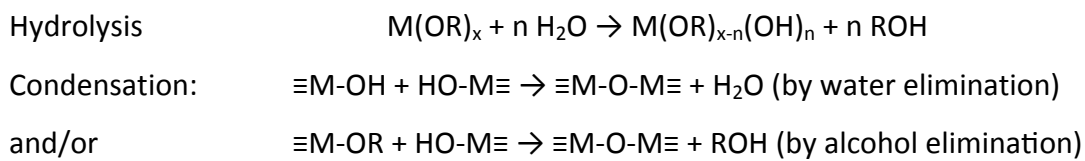
Nowadays, fiber reinforced concrete is widely used in the many civil engineering applications (e.g. industrial pavements, tunnel linings, marine structures, earthquake-resistant structures, etc). Due to the addition of fibers, plain concrete can be transformed from brittle into a ductile material, thus improving the resistance to crack formation and propagation. In particular, fiber-reinforced cementitious composites (FRCC) have been widely used, although the use of macro synthetic fibers made of polymeric materials has been proposed only recently for structural purposes [1]. For instance, the use of polypropylene-based fiber reinforced concrete (PFRC) has been encouraged for the design of road pavement in order to prevent micro- and macro-cracking due to drying shrinkage and fatigue phenomena [2]. Moreover, experimental tests performed by Lanzoni et al. [3] show that the addition of polypropylene-based draw-wired fibres significantly improves the crack resistance of the concrete mixture, thus enhancing toughness and durability of FRC structural components. At the same time, such improvement is attained without significantly affecting the workability of the mixture.

It is well known that the ductility and flexural strength of FRCC are determined by energy-dissipation mechanisms related to the pullout of the fibers, which depends on the bonding properties between fiber and matrix [4, 5]. However, with respect to other kinds of fibers, polypropylene (PP) macro synthetic fibers have the limitation of poor adhesion to the surrounding cement matrix due to their chemical inertness. The aim of the present work is to propose an innovative methodology for the improvement of the interfacial characteristics between PP macro synthetic fibers and cementitious matrices, validated by the results of pullout tests on single fibre.

The quality of the interface transition zone (ITZ) between the fiber and the matrix, and hence the bond strength, strongly depends on the extent of porosity in this area. Several studies have shown that microfillers e.g. microsilica (shotcrete application) added to cementitious composites may be employed to promote hydration and to decrease porosity [6]. The present study is inspired by the idea of implanting these densification agents directly on the surface of the PP macro synthetic fibers through a sol-gel treatment [7]. A surface nano-treatment has been proposed first in [7] for PP microfibers that can be employed mainly for reducing drying shrinkage in concrete. In the present work, a similar nano-treatment is proposed for macrofibers that can be added to the concrete mixture also for structural applications of FRC.

The sol-gel process, a chemical technique to synthesize inorganic materials, was initially employed to prepare high purity inorganic networks such as glasses and ceramic materials [8, 9].

This method is characterized by mild conditions, which become a strategic point when organic materials are involved into the process permitting to avoid their thermal degradation. Typical precursors are metal (or non metal) alkoxides, which react with water in the presence of an adequate basic catalyst and allow appearance to nanoparticles having narrow grain size distribution with dimensions ranging between 5 and 100 nm. The aqueous sol-gel reaction is generally divided into two steps: the first one named hydrolysis, when hydroxyl groups are produced, and the second one named condensation, when the polycondensation of hydroxyl groups and residual alkoxy groups to form a three-dimensional network are involved as follows:



Tetraethyl orthosilicate (TEOS) is a well studied alkoxide with chemical formula  $\text{Si(OR)}_4$ , where  $\text{R} = \text{C}_2\text{H}_5$  is the alkyl group. The mechanisms of hydrolysis and condensation reactions of silicon alkoxides involve bimolecular nucleophilic substitution reactions that can occur under either acid- or base-catalyzed conditions. Under acid-catalyzed conditions, the rate of hydrolysis is slow compared to the rate of condensation, which leads to longer polymer chains in the sol that continue to grow and entangle, occasionally cross-linking, until the gelation point is reached. In contrast, under base-catalyzed conditions, hydrolysis occurs rapidly, resulting in more highly branched clusters that do not readily interpenetrate and thus behave as discrete nano-structured species [10-12].

In this study, silica nanoparticles were deposited on PP fibers by sol-gel synthesis using ammonia as the basic catalyzer. The consequent interfacial bond enhancement was then investigated by performing pullout tests on single fiber, which provided the load–displacement relationship for a single fiber pulled out from the matrix. The behavior of treated and untreated macro synthetyc fibers was then compared by considering the maximum load and the pullout energy absorbed. Both parameters can be extracted from the results of the tests.

## **2. MATERIALS AND METHODS**

### **2.1. Fibers and treatment methods**

The macro synthetic fibers consist of PP monofilaments with a diameter of 0.78 mm (Figure 1) and length ranging from 30 to 60 mm. The main properties of the used PP fibers are reported in Tab. 1.

The materials used for the sol-gel treatment are ethanol (EtOH), ammonium hydroxide solution (NH<sub>4</sub>OH, ≈28 wt%) and tetraethyl-orthosilicate (TEOS). All materials are high purity reactants (Sigma-Aldrich) and have been used without any purification.

The chemical deposition has been obtained as follows. PP macro synthetic fibers were dipped in a 250 ml flask containing EtOH (120g), distilled water (12g) and NH<sub>4</sub>OH (18g) maintained at 60°C. After 10 min, TEOS (24g) was added into solution under magnetic stirring. After 2 hour, PP macro synthetic fibers were removed, washed with clean water and dried at room temperature.

### **2.2. Cement matrix**

Cement mortar with a mix proportion by weight of cement, sand and water C:S:W = 1:1.5:0.5 has been used for the experiment. The used cement was Portland Cement type CEM II/B – LL 32,5 R; the river sand with specific gravity of 2.69 Mg/m<sup>3</sup> had a particle size of 0-0,6 mm. The specimens were casted in plastic cylindrical molds and put to ripen at room temperature for 28 days.

### **2.3. Fiber and FRCC characterization**

In order to evaluate the morphology and distribution of SiO<sub>2</sub> nanoparticles on PP macro synthetic fibers surface, scanning electron microscopy (SEM) characterizations were performed with Nova NanoSEM 450 SEMFEG (FEI Company, USA). All images were acquired on the PP macro synthetic fibers surface in high vacuum with an In-lens SE detector (Through Lens Detector – Secondary electron mode, TLD-SE) and an accelerating voltage of 2KV. Chemical elemental analysis was carried out with an X-EDS QUANTAX-200 energy-dispersive X-ray spectroscopy system (Bruker, Germany).

To evaluate the interfacial bond enhancement due to the sol-gel treatment, pullout tests were performed on FRCC specimens. The test configuration (shown in Fig. 2) includes a single-side cement specimen. In order not to damage the fiber and to grip the fiber on the free side easier, the full length wire was used. One end of the wire was dipped in the cement sample for a length  $L_e$ , the other end of the wire was dipped in a resin capsule for a length much greater than  $L_e$ . In addition, in the latter part, two knots were practiced in order to avoid slip between wire and resin

[13, 14]. The cement specimen has cylindrical shape with both diameter and length of 80 mm. The diameter of the ring hole is 60 mm, so that no compressive stresses is produced nearby the fiber as a result of arch action [6]. Tests were carried out by an electro-mechanic traction machine under displacement control. The load cell is a GALDABINI 514262 TYPE TCA, OUTPUT 2mV/V with a capacity of 250 N and with an high accuracy class. The displacement control was performed by the actuator, at a rate of 1 mm/min.

The pullout test presented here can be divided into two main groups according to the embedded length as reported in Tab.2: the first group consists of six specimens with an embedded length  $L_e$  of 20 mm (sample code PP2 and PPT2); the second one consists of six specimens with an embedded length  $L_e$  of 30 mm (sample code PP3 and PPT3). In each group there are three samples with treated fibers (PPT) and three samples with untreated fibers (PP).

### 3. RESULTS

#### 3.1. SEM and EDX characterization

The SEM images of both untreated and sol-gel treated PP fibers are reported in Fig. 3 before they were embedded in the cementitious matrix for the pull-out test. Untreated PP macro synthetic fibers show a relatively smooth surface (Figs. 3a, 3c and 3e) even if a preferential orientation of the polymeric material is visible, probably due to the fiber extrusion process. SiO<sub>2</sub> nanoparticles can be observed on the surface of the treated PP macro synthetic fibers (see Figs. 3 b, 3d and 3f). These particles are spherical and the grain size distribution is quite narrow with mean diameter of about 50 nm. The nanoparticle distribution on the treated macro synthetic fibers is not uniform, since the nanoparticles tend to agglomerate and to form large islands that seem to consist of a single layer of silica nanoparticle. SiO<sub>2</sub> nanoparticles arrangement on the PP surface seem to follow the preferred orientation of the polymeric material.

The chemical composition of nanoparticles was confirmed by EDX spectra (Fig. 4) that show the presence only of silicon, oxygen, and carbon on the treated PP macro synthetic fibers.

The fibers after the pullout test are shown in Fig. 5. Therein, the diversity in the degree of abrasion between treated fibers (a) and untreated fibers (b) can be observed directly. The effect of abrasion seems to be more pronounced on the treated fiber than on the untreated fiber. In particular, the outer diameter of the untreated fibre is almost unchanged, whereas the outer surface of the treated fibers was clearly peeled during the pullout process. This phenomenon is responsible of the increase in the frictional stress observed during the pullout of treated fibers.

Finally, the related SEM images of the abraded surfaces of the fibres taken after that the pullout tests were completed are reported in Fig. 6. Comparison of the SEM images shows notable difference in the surface microstructure of the two specimens. In particular, scratches caused by the pullout process can be observed on the surface of the untreated sample (Figs. 6a, 6c and 6e), produced at the few points where the matrix has been able to grip the fiber mechanically. Moreover, few residual micrometric particles (white spots) of the cement matrix can be observed on the surface of the untreated fibers as a consequence of the weak chemical and mechanical bonding between the untreated PP fibre and the cementitious matrix.

Differently, the treated fiber after the pullout test seems to be circumferentially peeled and displays an homogeneous surface with some residual particles of cement matrix (Figs. 6b, 6d and 6f). Note that these matrix particles penetrate so much in deep into to the fiber surface that they are still bonded to the fibre even after the peeling of the fibre surface occurred during the pullout process.

### 3.2. Pullout diagrams

The pullout tests were conducted after 28 days from the date the cement samples casting. The differences in the load–displacement curves between treated and untreated fibers are shown in Figs. 7 and 8, for an embedded length  $L_e = 20$  mm.

The measured values of the maximum load and energy are reported in Table 3 together with the average peak load and average pull out energy. It can be seen that there is a factor of about 2 between the peak loads of treated and untreated fibers, and the ratio increases to 3 in terms of energy pullout. Similar results are shown in Figs. 9 and 10 for the specimens with an embedded length  $L_e$  of 30 mm, where the ratio between treated and untreated fibers provides a factor of 2.2 for the peak load and of 2.6 for the pullout energy.

Previous studies noted that the complete fiber pullout generally takes places in two phases: first, fiber debonding occurs along the entire length  $L_e$ , then a frictional behavior is observed during fiber pullout [6]. The contribution of creep of the PP fibre should also be taken into account during the entire process. Indeed, the final length of the fibre after the pullout process turns out to be slightly greater than the initial length  $L_e$ , being the elongation larger if  $L_e$  and thus the required pullout load are greater (Figs. 8 and 10).

It must be highlighted that synthetic and metal fibers display different behavior in the pullout phase after full debonding [15-18]. While the load-displacement diagram for the pull-out test of a

single metal fibers display a softening behavior due to an almost constant frictional shear stress [18], synthetic fibers show instead a hardening type behavior produced by the increase in the frictional shear stress with the fiber slip [19]. The abrasion phenomena at the outer surface of the fiber during the pullout are responsible of the pull-out hardening behavior, and the higher is the rate of abrasion the higher is the peak of the curve in the pullout diagram [16]. Pull-out hardening behavior is a very desirable property in FRCC, since it is generally accompanied by large energy absorption capacity [20]. As it can be observed from the shape of the curves in Figs 7-10, the obtained experimental results confirm qualitatively this kind of behavior.

Referring to the slip hardening interface behavior, it can be noted from the obtained peak values and the shape of the curves that the sol-gel nano-treatment remarkably improves the bond characteristics, both in the debonding and pullout phases.

In the absence of silica nanoparticles, the cementitious matrix do not interact with PP fiber surface due to the different surface energy. In treated fiber (PPT samples), nano-silica acts as a primer and the silanol groups on nanoparticles surface allows to produce hydration products, leading to improve the interfacial adhesion properties of PP fibers with the cementitious matrix.

#### **4. CONCLUSIONS**

The present work aims at improving the bond characteristics of PP macro synthetic fibers which, despite a poor interfacial bond strength, have seen an increase of their commercial attractiveness in recent years. Improvement of the adhesion characteristics becomes necessary in order to take full advantage of the properties of PP macro synthetic fibers embedded in the cement matrix.

Referring to the slip hardening interface behavior, from the obtained peak values and the shape of the diagrams it can be seen that the sol-gel nano-treatment remarkably improves the bond characteristics, both in the debonding and pullout phases. The improvement in the debonding phase is reflected by the increase (about double) of the full debonding load and this means that the densification of the ITZ, produced by the treatment, yields an increase in the maximum shear stress required for the full debonding (complete rupture of the ITZ in the whole  $L_e$  length ).

The improvement in the pullout phase is proved by the pullout energy required for the complete extraction of the fiber. In fact, the curves for treated fibers are steeper, thus meaning that the rate of abrasion is more severe. This result can be explained by the presence of the



hydration products in the ITZ that increase the stiffness locally, thus giving a remarkable increase in the frictional shear stress. In fact, the hydration products resulting from  $\text{SiO}_2$  activity improve the chemical interaction between the two phases and act as physical anchors as well.

The method of surface treatment here proposed offers new opportunities to FRCC by increasing the residual strength after FRCC first cracking as well as the energy absorption during post-cracking behavior, both being essential issues in the characterization of concrete composites by means of bending tests [4]. Since the post-cracking behavior is mainly influenced by energy absorption phenomena occurring during the fibre pullout, a significant increase of the residual strength after FRCC first cracking can be expected from bending tests performed on structural components made of FRCC with treated fibres, according to the European standard [21].

It can be excluded that the surface treatment may cause such an excessive improvement in fiber bond that it could lead to fiber breakage during bending tests. Indeed, untreated PP has very poor adhesion to the cementitious matrix as established by several studies [22] and no fiber breakage has ever been observed in FRCC in the present study as well as in pullout tests on fibers produced through a crimping process [23]. Since fiber breakage does not occur for continuously anchored fibers, then it is reasonably excluded also for fibres subject to nano treatment structured in islands. In conclusion, the nano-treatment here proposed can be considered as a more efficient and less disturbing alternative to the usual mechanical treatments that can originate pre-stresses in the material and consequently a reduction of its mechanical properties.

Finally, it can be observed that the framework proposed by Levin and Sevostianov [24] and more recently by Sevostianov et al. [25] for polymeric composite materials with inclusions and/or cracks can be efficiently employed in order to define the effective mechanical and rheological properties of this kind of FRCC. Moreover, the present study will be extended in a forthcoming article by performing proper engineering tests on large specimen carried out in compliance with the standards UNI EN 14651 [21], in order to demonstrate that the proposed nano-treatment does improve the engineering performance of structural components.

## **ACKNOWLEDGEMENTS**

Financial support from “Fondazione Cassa di Risparmio di Modena” within the Applied Research Project 2013/2014 “Carbon fibres and IPN resins” (convention C15414 prot. 182.14.8C) is gratefully acknowledged.

## REFERENCES

- [1] Bernard ES. Design of fibre reinforced shotcrete linings with macro-synthetic fibres. In: Amberg F, Garshol KF, editors. Shotcrete for Underground Support XI, Engineering Conferences International, Symposium Series, Volume P11, 2009, <http://dc.engconfintl.org/shotcrete/14>.
- [2] Nobili A, Lanzoni L, Tarantino AM. Experimental investigation and monitoring of a polypropylene-based fiber reinforced concrete road pavement. *Construction and Building Materials* 2013;47:888-895.
- [3] Lanzoni L, Nobili A, Tarantino AM. Performance evaluation of a polypropylene-based draw-wired fibre for concrete structures. *Construction and Building Materials* 2012;28.1:798-806.
- [4] Di Prisco M, Plizzari G, Vandewalle L. Fibre reinforced concrete: new design perspectives, *Materials and Structures* 2009;42:1261-1281.
- [5] Radi E, Di Maida P. Analytical solution for ductile and FRC plates on elastic ground loaded on a small circular area. *Journal of Mechanics of Materials and Structures* 2014;9.3:313-331.
- [6] Cunha VMCF, Barros JAO, Sena Cruz JM. Pullout behavior of steel fibers in self-compacting concrete, *Journal of Materials in Civil Engineering* 2010;22:1-9.
- [7] Yang Z, Liu J, Liu C, Zhou H. Silica modified synthetic fiber for improving interface property in FRCC. In: Barros JAO, editor. 8th Rilem International Symposium on Fiber reinforced Concrete: challenge and opportunities (BEFIB2012), Bagnex, France: RILEM Publications SARL; 2012, p. 347-357.
- [8] Brinker CJ, Scherer GW. *Sol-gel science: the physics and chemistry of sol-gel processing*. San Diego: Academic Press; 1990.
- [9] Hench LL, West JK. The sol-gel process. *Chemical Reviews* 1990;90:33-72.
- [10] Matijevic E. Monodispersed colloids: art and science. *Langmuir* 1986;2:12-20.
- [11] Brinker CJ, Mukherjee SP. Conversion of monolithic gels to glasses in a multicomponent silicate glass system. *Journal of Materials Science* 1981;16:1980-1988.
- [12] Sakka S, Kamiya K. Glasses from metal alcoholates. *Journal of Non-Crystalline Solids* 1980;42: 403-421.
- [13] Aiello MA, Leuzzi F, Centonze G, Maffezzoli A. Use of steel fibres recovered from waste tyres as reinforcement in concrete: Pull-out behaviour, compressive and flexural strength. *Waste management* 2009;29:1960-1970.
- [14] Weiler B, Grosse C. Pullout behaviour of fibers in steel fiber reinforced concrete. *Otto Graf Journal* 1996;7:116-127.

- [15] Zhong L, Li VC. Crack bridging in fiber reinforced cementitious composites with slip-hardening interfaces. *Journal of the Mechanics and Physics of Solids* 1997;45:763-787.
- [16] Li VC, Chan YW, Wu HC. Interface Strengthening Mechanism in Polymeric Fiber Reinforced Cementitious Composites. In Brandt AM, Li VC, Marshall LH, editors. *Proceedings of International Symposium on Brittle Matrix Composites 4 (BMC4)*. Warsaw: Ike and Woodhead Publishing; 1994, p. 7-16.
- [17] Li VC, Stang H. Interface Property Characterization and Strengthening Mechanisms in Fiber Reinforced Cement Based Composites. *Journal of Advanced Cement Based Materials* 1997;6:1-20
- [18] Modelling of fiber pull-out from a cement matrix. *International Journal of Cement Composites and Lightweight Concrete* 1988;10:143-149.
- [19] Li VC, Wang Y, Backer S. Effect of inclining angle, bundling and surface treatment on synthetic fibre pull-out from a cement matrix. *Composites* 1990;21.2:132-140.
- [20] Naaman AE, Reinhardt HW. High performance fiber reinforced cement composites. In: Shi C, Mo YL, editors. *High-performance construction materials. Science and Applications*, Singapore: World Scientific Publishing; 2008, p. 91-153.
- [21] UNI EN 14651. Test method for metallic fibre concrete. Measuring the flexural tensile strength (limit of proportionality (LOP), residual). European Committee for Standardization, B-1050 Brussels, September 2007.
- [22] Sehaj S, Shukla A, Brown R. Pullout behavior of polypropylene fibers from cementitious matrix. *Cement and Concrete Research* 2004;34:1919-1925.
- [23] Bentur A, Peled A, Yankelevsky D. Enhanced bonding of low modulus polymer fibers-cement matrix by means of crimped geometry. *Cement and concrete research*. 1997, 27.7: 1099-1111.
- [24] Levin V, Sevostianov I. Micromechanical modeling of the effective viscoelastic properties of inhomogeneous materials using fraction-exponential operators. *International Journal of Fracture* 2005;134:L37-L44.
- [25] Sevostianov I, Levin V, Radi E. Effective viscoelastic properties of microcracked materials: application of Maxwell homogenization scheme. *Mechanics of Materials* 2015; In press. doi:10.1016/j.mechmat.2015.01.004.

**TABLES**

Diameter [mm]	0.78
Lenght [mm]	30-60
Tensile Strenght [MPa]	500
Elastic Modulus [GPa]	4

**Tab.1 Characteristics of PP fibers**

Specimen	Fibre Type	L <sub>e</sub> [mm]
PP2.1	PP	20
PP2.2	PP	20
PP2.3	PP	20
PPT2.1	PPT	20
PPT2.2	PPT	20
PPT2.3	PPT	20
PP3.1	PP	30
PP3.2	PP	30
PP3.3	PP	30
PPT3.1	PPT	30
PPT3.2	PPT	30
PPT2.3	PPT	30

**Tab.2 Test specimens**

	Max Load [N]	Mean Value [N]	Energy [Nmm]	Mean Value [Nmm]
<b>PP2.1</b>	15,30	14±2	147,40	142±3
<b>PP2.2</b>	12,75		138,42	
<b>PP2.3</b>	15,00		142,49	
<b>PPT2.1</b>	32,65	30±4	450,44	437±50
<b>PPT2.2</b>	24,95		359,78	
<b>PPT2.3</b>	34,38		503,13	

**Tab.3 results of single fiber pullout for L<sub>e</sub> = 20 mm**

	Max Load [N]	Mean Value [N]	Energy [Nmm]	Mean Value [Nmm]
<b>PP3.1</b>	26,35	35±5	457,28	664±137
<b>PP3.2</b>	37,23		729,99	
<b>PP3.3</b>	43,58		804,62	
<b>PPT3.1</b>	67,20	79±8	1554,81	1732±120
<b>PPT3.2</b>	84,85		1898,39	
<b>PPT3.3</b>	84,65		1743,14	

**Tab.4 results of single fiber pullout for L<sub>e</sub> = 30 mm**